RESEARCH ARTICLE | JULY 15 2025

Simulation of small power wind turbine with vertical axis of rotation in framework of comsol

M. M. Hamdamov

AIP Conf. Proc. 3256, 040039 (2025)
https://doi.org/10.1063/5.0267762

Simulation of Small Power Wind Turbine With Vertical Axis of Rotation in Framework of Comsol

M. M. Hamdamov[1, 2, a)]

[1]*Institute of Mechanics and Seismic Stability of Structures named after M.T.Urazbaev, AS RUz, Tashkent, Uzbekistan*
[2]*Oriental University, Tashkent, Uzbekistan*

[a)] Corresponding author: mmhamdamov@mail.ru

Abstract. This paper presents the results of a $k-\varepsilon$ turbulence model for a rectangular airfoil problem using standard Comsol Multiphysics solvers. Flow around a rectangular airfoil was studied at Reynolds numbers of 10 000 < Re < 2 000 000 and angle of attack α = 0°–20°. Results were obtained for speed, pressure, and other parameters for different angle values. Implementing the Comsol Multiphysics software package showed good convergence, stability, and high accuracy of the model.

Keywords: Navier–Stokes equations, Comsol Multiphysics, Reynolds number, mass transfer process, turbulence model.

INTRODUCTION

In recent years, the Republic of Uzbekistan has adopted a set of measures aimed at further increasing the efficiency of electrical energy use in the economy and everyday life sectors, the widespread introduction of energy-saving technologies, and the development of renewable energy sources.

Over the past 50 years, 85% of the electricity generation in the republic corresponds to natural gas. The carbon dioxide and carbon oxides emitted from the combustion of hydrocarbons lead to atmospheric pollution, a decrease in its transparency, and an increase in turbidity. This, in turn, enhances the "greenhouse effect", which has increased the average temperature of the Earth's atmosphere by 1.5-2 degrees over the past hundred years. Such global climate change leads to melting the glaciers of the north and south poles of the Earth and the frequent formation of anomalous climatic phenomena. Ultimately, this is reflected in the planet's global ecological state and civilization's development. In this regard, today, the widespread use of alternative sources of electricity is becoming relevant [1-5].

Of the alternative sources of electricity, the cheapest and most environmentally appropriate is the driving force of the wind, which has a high economic indicator.

In general, by 2030, the development of a total wind power capacity of up to 5000 MW is predicted in Uzbekistan.

All this is about big energy. The government also supports small-scale power generation. Evidence of this judgment, particularly, is the financing, development, and implementation of low-power wind turbines with a vertical axis of rotation.

A wind turbine with a vertical axis of rotation is justified because wind turbines with high power start working from 7 m/s wind speed. Such wind speeds in Central Asia are achieved at high altitudes due to the area's areography or certain regions, for example, in the Akhangaran valley or in the coastal zones of the oceans. Thus, in the Republic of Uzbekistan, the wind potential refers to low wind speeds [6-10].

Hydrodynamic singularity methods, which use the distribution of singularities over the surface of an aircraft, have found wide application in the calculation of complex spatial flows. The flow parameters at a given point are determined by integrating 42 disturbances from all features. This integration is carried out numerically [10-15, 16]. If you select a final section of the surface, then under certain conditions, you can analytically integrate the influence of features located in the selected section. In this case, we come to the panel calculation method. Panel methods are convenient, for example, when considering local variations in the surface of an aircraft. Then, on panels not included in the modification zone, disturbances can be integrated only once for the original version, saving calculation time on an electronic computer (computer). However, the analytical calculation of integrals of distributed features

Water, Energy and Food Security in the Context of Global Climate Change and Water Scarcity
AIP Conf. Proc. 3256, 040039-1–040039-10; https://doi.org/10.1063/5.0267762
Published under an exclusive license by AIP Publishing. 978-0-7354-5198-8/$30.00

imposes restrictions on the shape of the panel and the type of approximation of the feature density distribution function. For example, in the known method [17], the wing panels must have parallel side edges and be flat. These requirements lead to a significant schematization of the aircraft's surface at the interfaces of the layout elements. The software package [18,19] uses arbitrary quadrangular panels as elements of a hyperbolic surface with a quadratic dipole distribution. The disturbance fields from such panels are described by complex analytical expressions, which require significant time and resources when calculating on a computer.

When distributing vortices and sources over the surface of load-bearing elements, the principle of symmetrization of features proposed in [20] is used to calculate the flow around profiles. Here, this principle is extended to the three-dimensional case. Let us first consider the well-known method for calculating the flow around solid wings with linearization of the boundary conditions [17]. In this method, a layer of sources and vortices was located in the base plane of the wing. The density of the sources was set to be proportional to the slopes of the half-thickness line of the profiles, and the circulation of the vortex layer was determined from the condition of non-flow of the middle surface of the wing. Let's divide the layer of sources and vortices into two equal parts and place these parts on the upper and lower surfaces of the wing. The intensity of the sources and vortices will be determined from the non-flow conditions, which will be satisfied at the control points of the panels distributed over the wing's surface. Naturally, the number of panels on the top and bottom surfaces should be the same, 44, but the sizes of the panels may differ. Let us recall that the density distribution of vortices is piecewise linear, and that of sources is piecewise constant. Just like in all panel methods, the problem is reduced to solving a system of linear equations for unknown intensities of features [17–20]. After solving the system, the velocities at the control points of the panels are calculated, and the pressure values and the total aerodynamic characteristics are determined.

The method of symmetrical singularities allows you to calculate thin and thick wings. In the limiting case of an infinitely thin lifting surface, it continuously transforms into the well-known calculation scheme with the distribution of vortices over the middle surface of the wing. In this case, the source layer degenerates, and its intensity tends to zero.

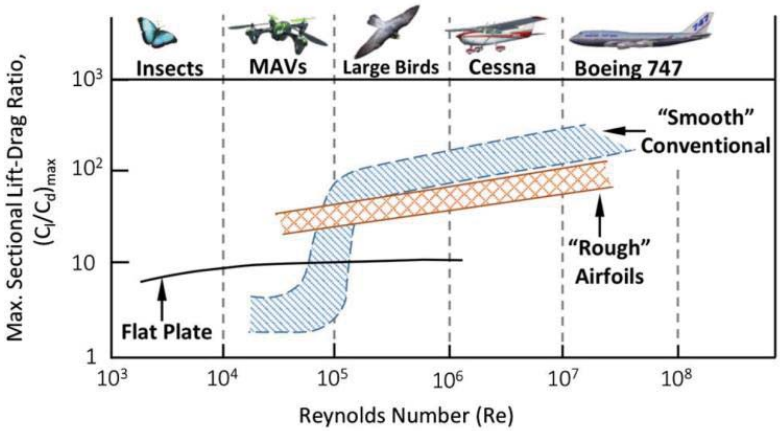

FIGURE 1. Influence of Reynolds number on maximum aerodynamic efficiency of profile section.

The finite element method was used to numerically solve the system of initial unsteady equations and the $k-\varepsilon$ turbulence model. Standard COMSOL Multiphysics 6.1 solvers were used for the solution.

Wind energy is a low-density energy source. Maximizing the efficiency of converting wind energy into mechanical forms of energy is critical to ensuring the economic efficiency of wind. Knowledge and understanding of rotor aerodynamics and blade shape design improve the overall performance of modern turbines. Wind turbine technology is based on the distribution of forces on the turbine rotor blades 3, caused by the mechanical torque on the shaft.

The shaft transmits torque from the blades to the generator. In modern wind turbines, the aerodynamic driving force is primarily lift rather than drag, as in ancient sailing ships.

Research conducted in this area has led to significant improvements in the overall efficiency of the energy conversion process. The ability to predict the updrafts of the flow field is an important factor in determining the interaction between turbines. Three approaches are available to analyze the flow around and downstream of wind turbines [14]:

Field tests give accurate results but is very complex and expensive;

Analytical and semi-empirical models, which make simplistic assumptions and are therefore not universally reliable;

Computational fluid dynamics (CFD) offers a better alternative to direct measurements.

This work aims to study the aerodynamics of a vertical axis wind turbine blade by numerically solving the governing equations using the finite volume method and the averaged Reynolds Navier-Stokes method.

Physico-mathematical formulation of the problem

A two-dimensional turbulent flow around a rectangular profile is considered. The physical picture of the flow under study and the configuration of the calculated fields are shown in Fig. 2.

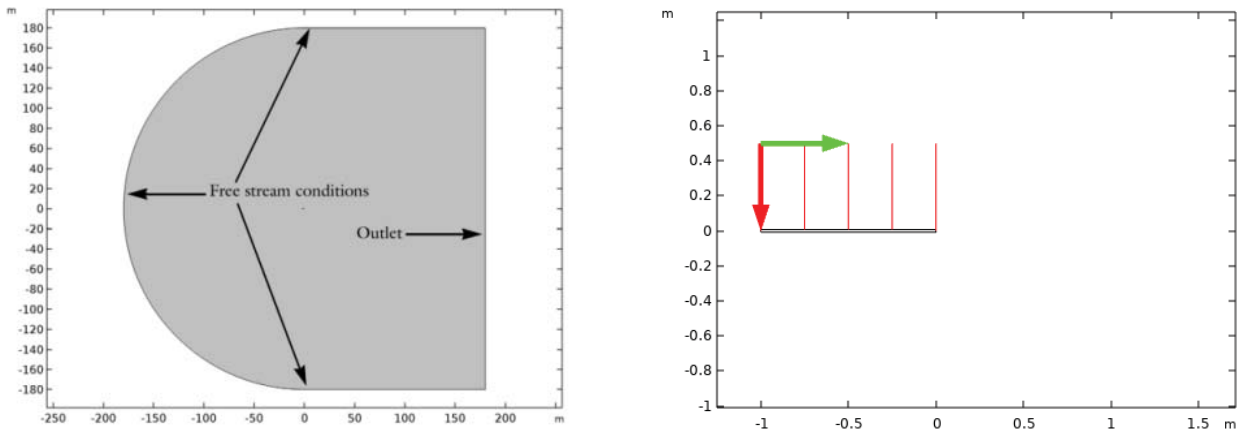

FIGURE 2. Scheme of computational domains: a) flow around profile b) profile geometry.

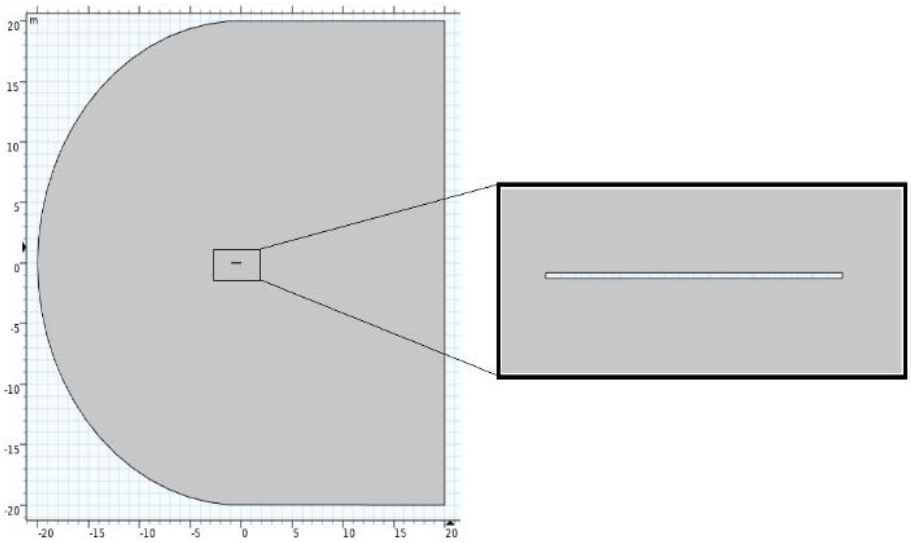

FIGURE 3. Profile geometry.

For a rectangular profile problem, the Reynolds number based on chord length is $10000<Re<2*10^6$. Chord length $c=1$ *m*. Two options for the angle of attack of the profile from $a=0$ *to* $a=20$ are considered.

Conservation equations. The general mass conservation equation or continuity equation can be written as follows (1).

$$\frac{d\rho}{dt} + \nabla\left(\rho\vec{v}\right) = 0 \tag{1}$$

where ρ is liquid density and $\vec{v}$ is velocity vector.

Equation of conservation of momentum. The general equation can be written as follows (2):

$$\frac{d}{dt}\left(\rho\vec{v}\right) + \nabla\left(\rho\vec{v}\right) = -\nabla_p + \nabla\overline{T} + \rho g + F \tag{2}$$

where p is static pressure, g and F are the force of the gravitational body and the external forces of the body (for example, arising during interaction with the dispersed phase), respectively.

Stress tensor $\overline{\overline{\tau}}$ in the following form (3):

$$\overline{\overline{\tau}} = \mu\left[\left(\nabla\vec{v} + \nabla\vec{v}T - \frac{2}{3}\nabla\vec{v}I\right)\right] \tag{3}$$

where μ is molecular viscosity, a I is unit tensor.

Reynolds and Navier-Stokes equations

The Reynolds-averaged Navier-Stokes (RANS) equations are time-averaged equations of motion for fluid flow. They are mainly used when working with turbulent flows. These equations can be approximated based on knowledge of the flow turbulence properties to obtain approximate average solutions of the Navier-Stokes equations. The equations can be written in Cartesian tensor form as (4), (5):

$$\frac{d\rho}{dt} + \frac{d}{dx_i}\left(\rho\vec{v}_i\right) = 0 \tag{4}$$

$$\frac{d}{dt}\left(\rho\vec{v}_i\right) + \frac{d}{dx_i}\left(\rho v_i v_j\right) = -\frac{dp}{dx_i} + \frac{d}{dx_j}\left[\mu\left(\frac{dv_i}{dx_i} + \frac{dv_j}{dx_j} - \frac{2}{3}\delta_{ij}\frac{dv_i}{dx_j}\right)\right] + \frac{d}{dx_i}\left(-\rho v_i v_j\right) \tag{5}$$

Equations (4) and (5) are called Reynolds-averaged Navier-Stokes equations, in which the velocities and other decision variables are now ensemble averages (or time averages). Given fluid velocity as a function of position and time, the average fluid velocity (6):

$$v_i = v_i + v_i' \tag{6}$$

The left frequency equation represents the change in the average momentum of the mass element due to the unsteadiness of both the average flow and convection to the average flow.

Laminar flows are characterized by low Reynolds numbers. The higher the Reynolds number, the more likely the flow is to be turbulent, and the less shallow lengths (mixing) there are in the flow. The Reynolds number gives a measure of the relative importance of inertial and viscous forces; for a wing, it is defined as:

To find out whether the flow is steady or turbulent, we need to calculate the Reynolds number

$$\mathrm{Re} = \frac{\rho u l}{\mu} = \frac{1.2043 \times 20 \times 1}{1.81397 \times 10^{-5}} = 1.327805 \times 10^6$$

As can be seen from this Re value, the turbulence becomes very large. Therefore, we should select a turbulent model representing this process and use it for this problem.

Modified model $k-\varepsilon$. Unlike well-known works, here it is proposed to use a modified $k-\varepsilon$ model, which contributes to a more adequate description of the heat and mass transfer process [15-19]:

$$\begin{cases} \dfrac{\partial}{\partial t}(\rho k)+\dfrac{\partial}{\partial x_j}(\rho k u_j)=\dfrac{\partial}{\partial x_j}\left[\left(\mu+\dfrac{\mu_t}{\sigma_k}\right)\dfrac{\partial k}{\partial x_j}\right]+G_k+G_b-\rho\varepsilon-2\rho\varepsilon M_t^2+S_k, \\ \dfrac{\partial}{\partial t}(\rho\varepsilon)+\dfrac{\partial}{\partial x_j}(\rho\varepsilon u_j)=\dfrac{\partial}{\partial x_j}\left[\left(\mu+\dfrac{\mu_t}{\sigma_\varepsilon}\right)\dfrac{\partial \varepsilon}{\partial x_j}\right]+\rho C_1 S\varepsilon-\rho C_2\dfrac{\varepsilon^2}{k+\sqrt{\nu\varepsilon}}+C_{1\varepsilon}\dfrac{\varepsilon}{k}C_{3\varepsilon}G_b+S_\varepsilon. \end{cases}$$

The notation used here is

$$C_1=\max\left[0.43,\frac{\eta}{\eta+5}\right],\ \eta=S\frac{k}{\varepsilon},\ S=\sqrt{2S_{ij}S_{ij}},\ \mu_t=\rho C_\mu\frac{k^2}{\varepsilon},\ C_\mu=\frac{1}{A_0+A_S\dfrac{kU^*}{\varepsilon}},\ U^*\equiv\sqrt{S_{ij}S_{ij}+\tilde{\Omega}_{ij}\tilde{\Omega}_{ij}},$$

$$\Omega_{ij}=\overline{\Omega_{ij}}-2\varepsilon_{ijk}\omega_k,\qquad A_S=\sqrt{6}\cos\phi,\qquad \phi=\frac{1}{3}\cos^{-1}\left(\sqrt{6}W\right),\qquad W=\frac{S_{ij}S_{jk}S_{ki}}{\tilde{S}^3},\qquad \tilde{S}=\sqrt{S_{ij}S_{ij}},$$

$$S_{ij}=\frac{1}{2}\left(\frac{\partial u_j}{\partial x_i}+\frac{\partial u_i}{\partial x_j}\right),\ G_k=-\rho\overline{u_i'u_j'}\frac{\partial u_j}{\partial u_i},\ S\equiv\sqrt{2S_{ij}S_{ij}},\ G_b=\beta g_i\frac{\mu_t\partial T}{\mathrm{Pr}_t\,\partial x_i},\ \mathrm{Pr}_t=1/a_t,\ a_0=1/\mathrm{Pr}=k/\mu c_p$$

$$,\ \beta=-\frac{1}{\rho}\left(\frac{\partial\rho}{\partial T}\right)_p,\ G_b=-g_i\frac{\mu_t}{\rho\,\mathrm{Pr}_t}\frac{\partial\rho}{\partial x_i},\ M_t=\sqrt{\frac{k}{a^2}},\ a=\sqrt{\gamma RT}.$$

Empirical constants $k-\varepsilon$ models take standard values: $C_{1\varepsilon}=1.44$, $C_2=1.9$, $\sigma_k=1.0$, $\sigma_\varepsilon=1.2$, $A_0=4.04$.

The $k-\varepsilon$ model is apparently the most successful model of first-level closure turbulence. To describe turbulent quantities, it uses a system of two nonlinear diffusion equations - for the mass density of turbulent energy k and the dissipation rate of turbulent energy ε. The simplest version of this model appeared more than thirty years ago. Since then, the k-ε model has been widely used to calculate various problems, mainly to describe shear incompressible turbulence.

Spalart-Allmaras model. This model belongs to the class of one-parameter linear turbulence models. Here, only one additional differential equation appears for calculating the kinematic coefficient of eddy viscosity. This low Reynolds turbulence model, which describes the entire flow region, is given by the following equation:

$$\frac{\partial}{\partial t}(\rho\tilde{\nu})+\frac{\partial}{\partial x_i}(\rho\tilde{\nu}u_i)=$$

$$G_\nu+\frac{1}{\sigma_{\tilde{\nu}}}\left[\frac{\partial}{\partial x_j}\left\{(\mu+\rho\tilde{\nu})\frac{\partial\tilde{\nu}}{\partial x_j}\right\}+C_{b2\rho}\left(\frac{\partial\tilde{\nu}}{\partial x_j}\right)^2\right]-C_{w1\rho}f_w\left(\frac{\tilde{\nu}}{d}\right)^2+S_{\tilde{\nu}}.$$

Turbulent eddy viscosity is calculated by the formula: $\mu_t=\rho\tilde{\nu}f_{\nu1}$, additional definitions are given by the following dependencies: $f_{\nu1}=\dfrac{\chi^3}{\chi^3+C_{\nu1}^3}$, $\chi=\dfrac{\tilde{\nu}}{\nu}$ $\tilde{S}\equiv S+\dfrac{\nu}{\kappa^2d^2}f_{\nu2}$, $f_{\nu2}=1-\dfrac{\chi}{1+\chi f_{\nu1}}$, $S\equiv\sqrt{2\Omega_{ij}\Omega_{ij}}$,

$\Omega_{ij} = \frac{1}{2}\left(\frac{\partial u_i}{\partial x_j} - \frac{\partial u_j}{\partial x_i}\right)$, $S_{ij} = \frac{1}{2}\left(\frac{\partial u_j}{\partial x_i} + \frac{\partial u_i}{\partial x_j}\right)$, $f_w = g\left[\frac{1+C_{w3}^6}{g^6+C_{w3}^6}\right]^{1/6}$, $r = \frac{\tilde{\nu}}{\tilde{S}\kappa^2 d^2}$, and the closure constants for the model are: $C_{prod} = 2.0$, $C_{b1} = 0.1355$, $C_{b2} = 0.622$, $\sigma_{\tilde{\nu}} = \frac{2}{3}$, $C_{\nu 1} = 7.1$, $C_{w1} = \frac{C_{b1}}{\kappa^2} + \frac{(1+C_{b2})}{\sigma_{\tilde{\nu}}}$, $C_{w2} = 0.3\, C_{w3} = 2.0$, $\kappa = 0.4187$.

SOLUTION METHOD

Time-averaged and normalized longitudinal velocity (or flow velocity) profiles allow the flow characteristics to be assessed at various points downstream of the profile. Profile normalization means that the flow values at each point are divided by the maximum flow value in that profile. Time-averaged and normalized longitudinal velocity profiles are evaluated at three points (x/c = 0, 0.25, 0.5, 0.75, and 1) behind the profile.

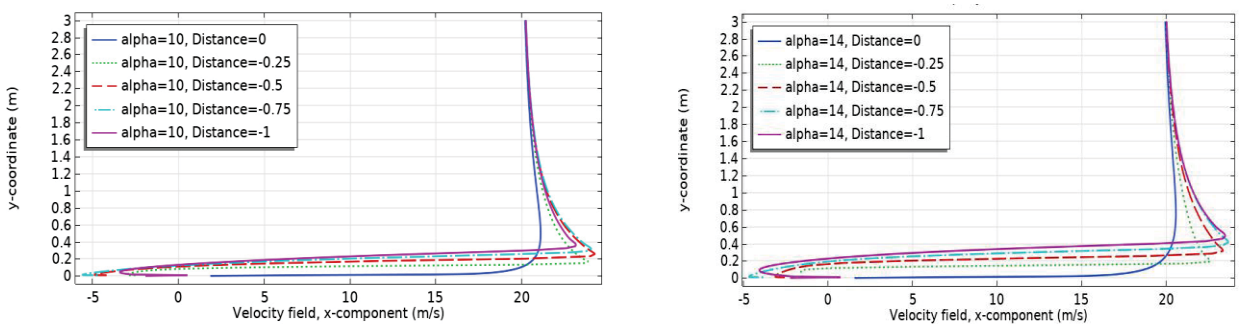

FIGURE 4. Longitudinal velocity field at sections x/c = 0, 0.25, 0.5, 0.75, 1.

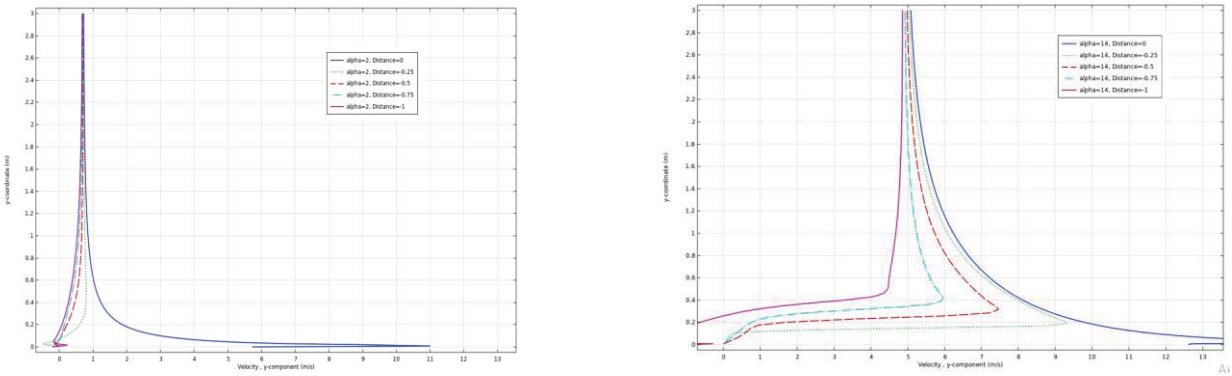

FIGURE 5. Transverse velocity field at sections x/c = 0, 0.25, 0.5, 0.75, 1.

The distribution of the surface pressure coefficient on the wing profile is characterized by a change in pressure on its surface depending on the distance from a certain point. Typically, the analysis uses the surface pressure coefficient (C_p), which is defined as the ratio of the pressure difference between a point on the profile surface and the free flow pressure to the dynamic free flow pressure.

$$C_p = \frac{p - p_\infty}{0.5\rho U_0^2}$$

where p is pressure at a point on the profile surface, P_∞ is free stream pressure, ρ is free stream density, U_0 is free stream speed.

On the charts C_p zones of positive and negative pressure are usually distinguished. The positive pressure zone is usually called the lift zone, and the negative pressure zone is called the resistance zone. The distribution of the surface pressure coefficient on the wing profile can be used to analyze its aerodynamic characteristics, such as lift, drag coefficient, etc. Fig. 13 - shows the distribution of the surface pressure coefficient Cp at angles of attack $\alpha = 0^0 \ldots\ldots 20^0$.

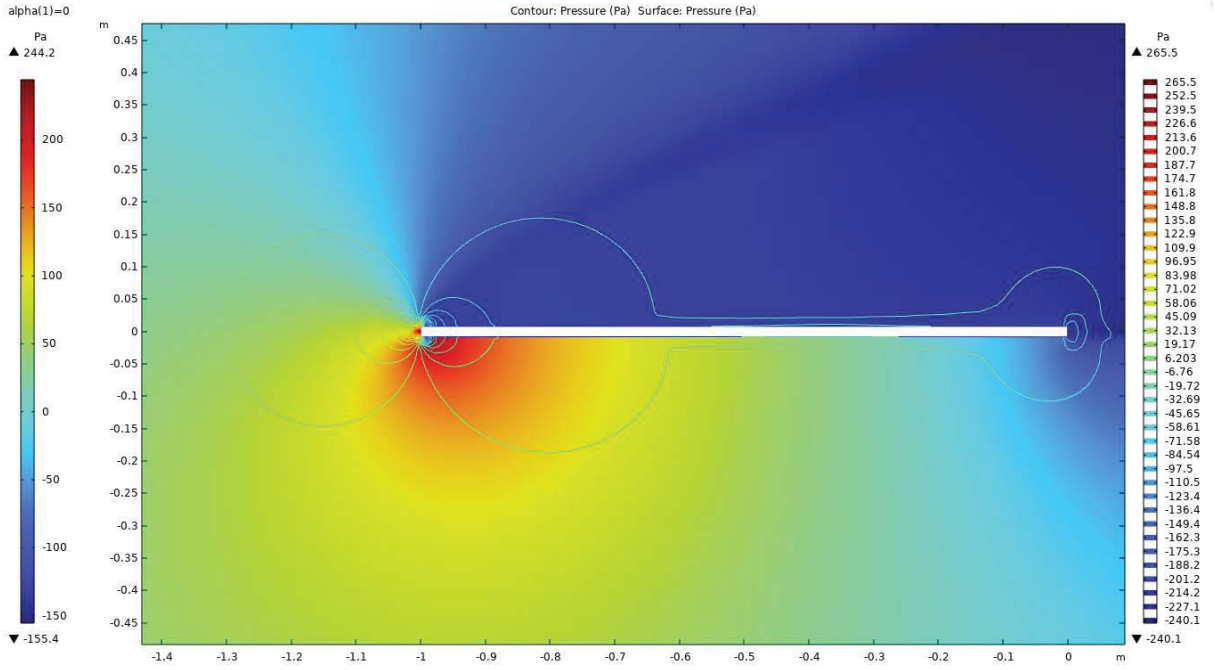

FIGURE 6. Pressure field at alpha = 0 deg.

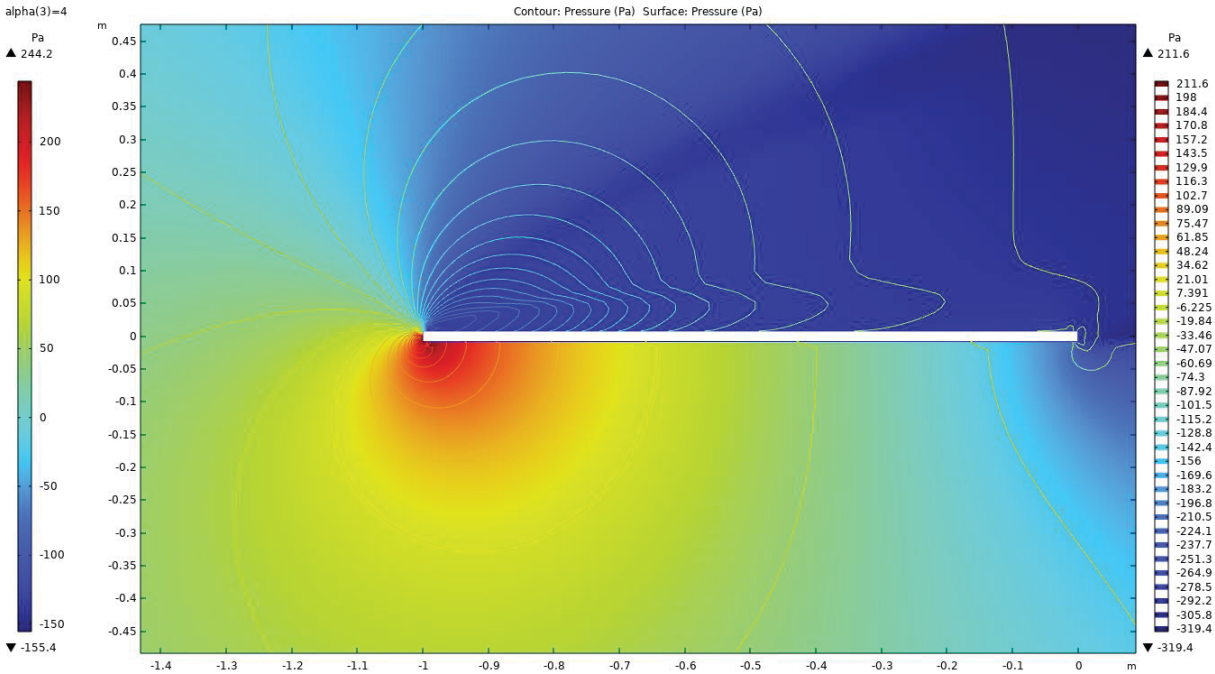

FIGURE 7. Pressure field at alpha= 4 degrees.

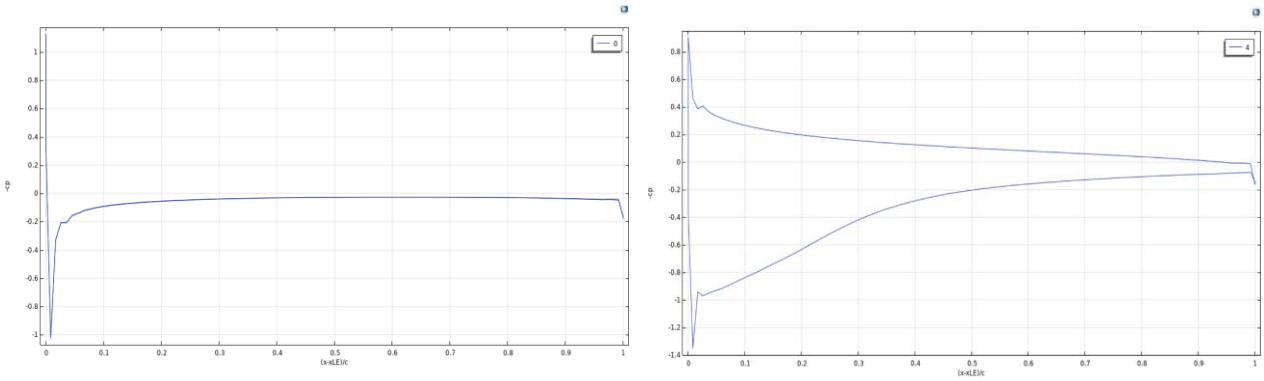

FIGURE 8. Surface pressure coefficient C_p

The distribution of the surface friction coefficient on an airfoil is characterized by a change in the friction force on its surface depending on the distance from a certain point.

The influence of the accuracy of boundary layer modeling on the accuracy of calculating the integral and distributed characteristics of the wing profile is studied using RAE 2822 as an example. Two mathematical gas flow models are used: k-ω SST and "inviscous" gas. The solution is carried out by algorithms of the first and second orders of accuracy, which give different results in the region of boundary layer separation. As numerical studies have shown, the accuracy of calculating the friction coefficient on the surface of the profile and the thickness of the boundary layer significantly affects the determination of the flow separation point, which affects the calculation of the pressure distributed over the surface and the integral characteristics of the profile [16-21].

The coefficient of surface friction C_f is defined as the ratio of the friction force acting on the surface of the profile to the dynamic pressure of the free flow.

$$C_f = \frac{F}{0.5\rho U_0^2 S}$$

where F is the friction force acting on the profile surface, S is the profile surface area oriented along the flow. Graphs of Cf are usually used to analyze the distribution of the surface friction coefficient on the wing profile depending on the distance from a certain point on the profile surface. On C_f graphs, zones of high and low friction are usually distinguished. The high friction zone is usually located in the area of the leading edge of the profile and in the area of flow separation on the upper surface of the profile, as seen in Fig. 9.

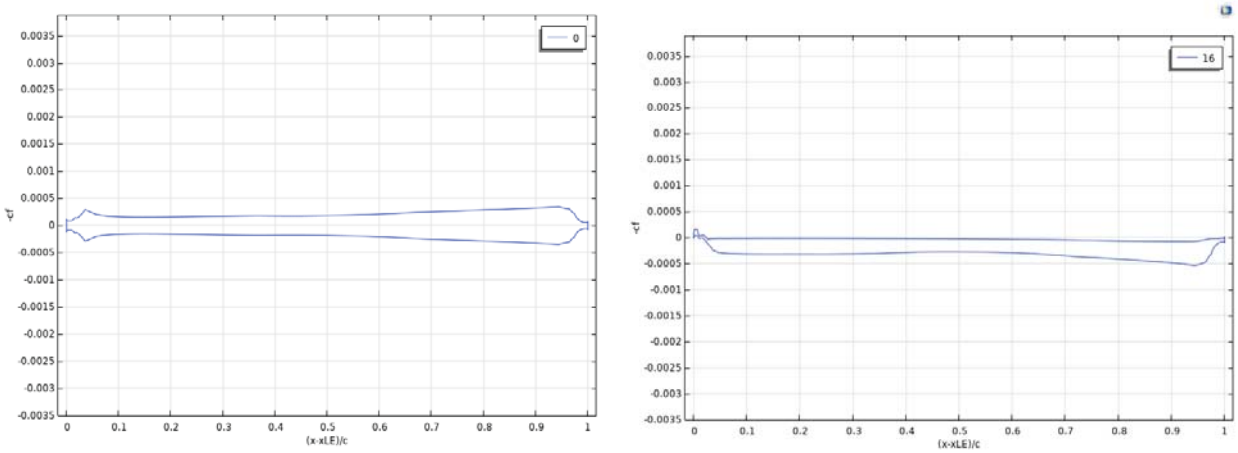

FIGURE 9. Surface friction coefficient C_f.

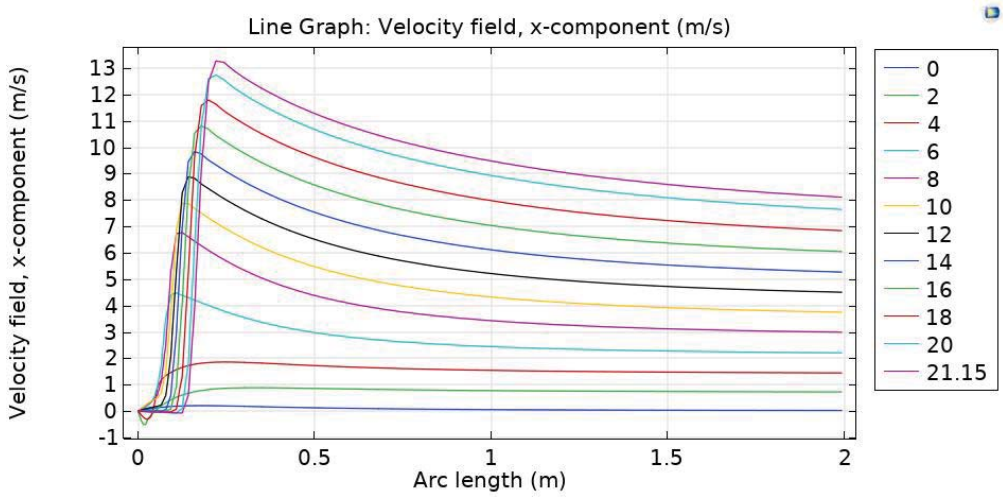

FIGURE 10. Velocity field at different alpha values.

CONCLUSION

The article presents numerical results of the turbulent flow of an incompressible fluid around a rectangular profile using the $k-\varepsilon$ turbulence model in the Comsol Multiphysics software package.

The accuracy of determining the separation point of the boundary layer depends on the reliability of modeling friction stresses on the wall; an erroneous determination leads to a distortion of the pressure coefficient and leads to errors in the integral characteristics. But, as practice shows, paying much attention to the accuracy of determining friction stresses is not always necessary. With continuous flow, its influence is small, and consequently, the choice of model to solve the problem is significantly easier.

REFERENCES

1. Liu, J., Lin, H., & Zhang, J. Review on the technical perspectives and commercial viability of vertical axis wind turbines. Ocean Engineering, 182, 608-626. (2019).
2. Solovyov A., Degtyarev K. Wind energy. Science and life. No. 7, (2013).
3. Energy portal. Issues of production, conservation and processing of energy. (2022).
4. Obukhov S.G. Electricity Generation Systems Using Renewable Energy Resources. Publishing House of Tomsk State University, (2008).
5. Martyanov, A. S. Research of control algorithms and development of a controller for a wind power plant with a vertical axis of rotation. Chelyabinsk, (2016).
6. Mezaal, N. A. Mathematical modeling of a wind power plant (WPP) with a capacity of 1.5 MW using computational fluid dynamics (CFD) in ANSYS. Chelyabinsk: SUSU, (2018).
7. D. MacPhee and A. Beyene. Recent advances in rotor design of vertical axis wind turbines, Wind Eng., vol. 36(6), pp. 647–666, (2012).
8. Versteeg, H. K. and W. Malalasekera, An introduction to computational fluid dynamics: The finite volume method. (2007).
9. Oganesyan E.V., Bekirov E.A., Asanov M.M. Matematicheskaya model dlya opredeleniya parametrov raboti vetroenergeticheskoy ustanovki. Stroitelstvo I texnogennaya bezopasnost, Vol. 3 (55), pp.82-86. (2016).
10. Kaplya Ye.V. Matematicheskaya model perexodnix protsessov povorotno opastnoy Vetroenergeticheskoy ustanovki. Matem. modelirovaniye, Vol. 25(12). pp. 33–43. (2013).
11. Belotserkovsky, O.M. Large particle method in gas dynamics. Moscow, Science, (1982).
12. Fletcher, K. Computational methods in fluid dynamics. Vol. 1. Moscow, World, 1991.
13. Fletcher, K. Computational methods in fluid dynamics. Vol. 2. Moscow, World, 1991.
14. Peter A. Kozak, David Vallverdú, and Dietmar Rempfer. Modeling Vertical-Axis Wind-Turbine Performance: Blade-Element Method Versus Finite Volume Approach. Journal of propulsion and power Vol. 32(3), (2016).

15. Conyers, H. J., Dowell, E. H., & Hall, K. C. Aeroelastic studies of a rectangular wing with a hole: Correlation of theory and experiment. In 2010 Aerospace Systems Conference (No. SSTI-8080-0045). (2010).
16. Terekhin, A. A., Sidelnikov, R. V., & Terekhin, T. V. Numerical analysis of the influence of surface friction on the aerodynamic characteristics of an airfoil. Bulletin of the South Ural State University. Series: Mechanical Engineering, (10 (110)), 45-48. (2008).
17. Spalart, P.R., Allmaras, S.R. A one-equation turbulence model for aerody-namic flows. AIAA J. 92, 0349. (1992).
18. Hamdamov M. M., Ishnazarov A. I., Mamadaliev K. A. Numerical Modeling of Vertical Axis Wind Turbines Using ANSYS Fluent Software. Lecture Notes in Computer Science (including subseries Lecture Notes in Artificial Intelligence and Lecture, 13772 LNCS, p. 156–170, (2023).
19. Khujaev I.K., Fayziev R.A., Hamdamov M.M. Numerical Solution of the Combustion Process Using the Computer Package Ansys Fluent. Lecture Notes in Computer Science (including subseries Lecture Notes in Artificial Intelligence and Lecture, 13772 LNCS, P. 26–37, (2023).
20. Hamdamov M., Khujaev I., Bazarov O., Isabaev K. Axisymmetric turbulent methane jet propagation in a wake air flow under combustion at a finite velocity. In IOP Conference Series: Materials Science and Engineering, 1030(1), 012163 (2021).
21. Khujaev I.K., Hamdamov M.M. Axisymmetric turbulent methane jet Propagation in a co-current air flow under combustion at a finite velocity**.** Herald of the Bauman Moscow State Technical University, (5), pp.89–108 (2021).